SCIENTIFIC PAPER
Published: April 1, 2025
https://doi.org/10.13167/2025.30.7

Coir geosynthetics as a reinforcing material for pond ash used in road subgrade

Sujit Kumar Pradhan[1] and Goutam Kumar Pothal[1]

[1] Indira Gandhi Institute of Technology Sarang, Department of Civil Engineering, Dhenkanal, Odisha, Zip Code-759146, India

Corresponding author:
Sujit Kumar Pradhan
sujitpradhan@igitsarang.ac.in

Received:
July 16, 2024

Revised:
September 13, 2024

Accepted:
December 31, 2024

Published:
April 1, 2025

Citation:
Pradhan, S. K.; Pothal, G. K. Coir geosynthetics as a reinforcing material for pond ash used in road subgrade. *Advances in Civil and Architectural Engineering,* 2025, 16 (30), pp. 106-125. https://doi.org/10.13167/2025.30.7

ADVANCES IN CIVIL AND ARCHITECTURAL ENGINEERING (ISSN 2975-3848)

Faculty of Civil Engineering and Architecture Osijek
Josip Juraj Strossmayer University of Osijek
Vladimira Preloga 3
31000 Osijek
CROATIA

Abstract:
Woven coir geosynthetics are being investigated as a substitute for geosynthetics in reinforcement applications due to their exceptional technical properties. They are commonly used to strengthen pond ash, which can be substituted for soils that have a low load-bearing capacity. This lowers the overall expense for construction and reduces the demand for natural soil. In this study, three varieties of woven coir geosynthetics, designated as C1, C2, and C3, were used to reinforce pond ash. An experimental test was conducted on a model strip footing lying on pond ash reinforced with coir geosynthetics, focusing on variables such as the number of layers, depth of top reinforcement, and width of reinforcement. In addition, triaxial testing was performed on pond ash reinforced with C2 and C3, including variables such as confining pressure and the number of reinforcing layers. The findings suggest that the inclusion of woven coir geosynthetics significantly enhanced the strength and load-bearing capacity. When a single layer of reinforcement was used with fine pond ash, the performance of the C2 and C3 types of coir geosynthetics varied. However, when several layers of reinforcement were used, the C3 type demonstrated superior outcomes. Increasing the thickness of reinforcement layers and the containing pressure both enhanced the strength of the reinforced pond ash. Multiple regression analyses were performed to develop mathematical models. An analysis revealed a substantial relationship between the measured and predicted levels of ultimate bearing capacity ratio.

Keywords:
pond ash; coir geosynthetics; bearing capacity; settlement; mathematical model

1 Introduction

Owing to the significant impact of transportation infrastructure on a country's economy, ongoing endeavours are being undertaken to preserve road quality by implementing environmentally sustainable construction techniques, thereby decreasing future costs. Low-volume roads, which constitute more than half of the overall road network, are frequently given a lower priority than highways. More than 70 % of roads in countries like India, which has the second-largest road network in the world, are made up of low-volume rural routes [1]. A significant portion of India is characterised by expansive black cotton soils, commonly known as soft soils. Improvements in the strength of soft soil are necessary because of the significant increases in load-bearing demands, decreases in shear strength, extensive settling, and insufficient soil stability. A decrease in the shear strength of these soils can lead to inadequate support for structures making it very important to implement appropriate soil stabilisation processes.

Nevertheless, there is a persistent shortage of premium-grade natural soils. India's thermal power plants produce significant quantities of pond ash, which is a residual by-product of coal combustion. Pond ash is composed of fly ash and bottom ash, which are collected from ponds for disposal purposes. The scale of pond ash production and associated issues pose significant environmental and disposal challenges.

According to recent reports, Indian thermal power plants generate more than 150 million tonnes of ash annually. For instance, the Central Electricity Authority of India provides data indicating that in the 2021-22 fiscal year, approximately 172 million tons of ash will be produced [2]. This large quantity of pond ash is often stored in designated ash ponds or landfills, which can reach capacity and lead to land and water contamination.

Ash ponds can leach harmful chemicals, such as heavy metals and toxic elements, into the soil and groundwater, potentially affecting local ecosystems and human health. Studies have shown that the leachate from ash ponds can contaminate nearby water sources [3]. During dry periods, wind can cause the ash from these ponds to become airborne, leading to air pollution and respiratory issues for nearby populations.

The extensive land required to store pond ash can lead to conflicts over land use and limited space for other essential developments. The management and remediation of ash ponds involve significant costs, including the maintenance and monitoring of containment structures to prevent environmental contamination.

The Government of India published guidelines in May 2013 requiring State Governments to propose that at least 15 % of the total road length under the Pradhan Mantri Gram Sadak Yojana should use new technologies such as cement stabilisation, lime stabilisation, cell-filled concrete, and coir geotextiles to encourage the use of locally available materials. Geosynthetics composed of coir have been used to enhance the strength and characteristics of subgrade soil layers, and fill materials for road subgrades with enhanced bearing capacities have been made from pond ash reinforced with coir geosynthetics. This offers a solution to the problems of natural resource shortages and waste-material usage.

Geosynthetic foundation soil reinforcement has been recognised as a scientifically and economically viable solution for addressing the excessive settling and low-load bearing of soft soils, particularly for shallow foundations [4-6]. Several numerical and experimental studies have shown that the performance of foundation soil reinforced with geosynthetics can be influenced by several parameters, such as the reinforcement type, reinforcement layout, footing size and shape, and the geosynthetic interface [7-9].

According to Lal [10], coir geocells can distribute pressure over large depths. A previous study [11] shows an improvement in the bearing capacity of a square footing (with a width B of 800 mm) reinforced with jute geosynthetics under pond ash. Through triaxial compression testing, the effects of the reinforcement form on the strength improvement of geosynthetic-reinforced sand were examined. It has been found that the cellular type of reinforcement is more effective in enhancing strength than the planar form [12].

Tafreshi [13] conducted model experiments using planar-reinforced sand beds with similar geosynthetic properties and strip footings supported by geocells. The findings of this research showed that footing settlement and bearing pressure could potentially be alleviated using less geosynthetic material. The strength of soil samples is increased by about 1,10-1,37 times when coir fibres are added to expansive soils [14-16]. The foundation settlement can be reduced by strengthening the foundation using coir fibres [10, 17]. Researchers have suggested that the lifespan of coir makes it suitable for use as a reinforcing material based on the findings of durability investigations [18]. While coir and other natural fibre geotextiles are feasible for initial-stage applications and temporary roads, their suitability for road subgrades in more permanent settings remains limited unless used in combination with synthetic reinforcements or other protective measures. A previous study addressed the effect of adding coir material to soft clay [19]. Research has shown that using coir products increases the strength of soft soil. Laboratory model tests were conducted [20] to examine the impact of braided coir rope reinforcement on the pressure versus settlement behaviour of a square model footing founded on loose sand. The results revealed that the incorporation of one or more coir rope reinforcement layers significantly improved the load-carrying capacity of the model footing at all normalised settlement levels. Vinod [21] examined the undrained response of clay specimens reinforced with sand-coir fibre cores in triaxial testing (under optimal moisture content and maximum dry density (MDD) conditions). The stress–strain–strength behaviour of sand-coir fibre-reinforced clay specimens with fibre concentrations up to 3 % is much better than that of unreinforced clay specimens, which is one of the extremely encouraging aspects of the findings.

The inclusion of geosynthetics improves the mechanical characteristics of soil by increasing its peak strength and axial strain at failure and reducing strength loss after reaching its peak [22]. According to a previous study [23] on a strip footing sitting on a geocell-reinforced sand bed, the reinforced soil system behaved better up to a reinforcement length of approximately 4 x footing width, beyond which there was only a slight improvement. Sharma [24] explored how the bearing capacity of a foundation bed can be improved by layering geosynthetics. The optimum depths for embedding a single layer of geosynthetics and multiple layers of geosynthetics under the footing were found to be 0,3 x footing width and 0,5 x footing width, respectively. Geosynthetic-reinforced soil foundations have been extensively used to revitalise and strengthen soft soil foundations because they can increase the foundation's bearing capacity and decrease the footing settlement [25]. Polymeric and natural fibre geosynthetics significantly improve the strength of pond ash [26, 27].

Few studies have been conducted on the induction of coir geosynthetics in road subgrades. In this study, the strength behaviour, settlement rate, and bearing capacity of pond ash reinforced with woven coir geosynthetics were analysed. To achieve this, an extensive set of experimental tests was conducted to evaluate the effectiveness of strip footing in sustaining reinforced pond ash. In addition, mathematical models are developed to validate the experimental results.

2 Materials and methods

2.1 Materials

2.1.1 Coir geosynthetics

Geosynthetics made of woven coir were used as the reinforcement in this study. They were purchased locally from suppliers in Odisha. Three distinct types of woven coir geosynthetics, designated C1, C2, and C3, were used. These geosynthetics were selected not only because of their local availability but also because of their distinct physical properties, such as aperture size, tensile strength, and elongation behaviour, which are important for soil reinforcement applications.

C1 type geosynthetics has a wide open mesh structure with large apertures (25 x 25 mm) and a thickness of 6,5 mm. This allows for high water permeability and is suitable for applications

such as erosion control. However, it is unsuitable for fine particle filtration because of its large apertures. The C2 type has a medium mesh structure with smaller apertures than the C1 type (10,0 x 12,5 mm) and a thickness of 7,8 mm. It provides a balance between permeability and particle retention and is useful for applications involving moderate filtration and reinforcement. The C3 type is dense and tightly woven with no visible apertures (7 x 4 mm) and a thickness of 9,2 mm. It is suitable for fine particle filtration and separation and is used in drainage systems or as a barrier to prevent soil loss. Although it is less effective for applications requiring high water permeability, it is the most effective reinforcement.
The variation in the characteristics of C1, C2, and C3 allowed for a comparative study of their performance under different conditions, ensuring a comprehensive evaluation of their suitability for improving the bearing capacity and stability of reinforced pond ash (Figure 1). Table 1 lists the physical characteristics, tensile strength, and elongation at failure of the woven coir geosynthetics, and the physical properties of the pond ash. Figure 2 shows the tensile strength of the coir geosynthetics.

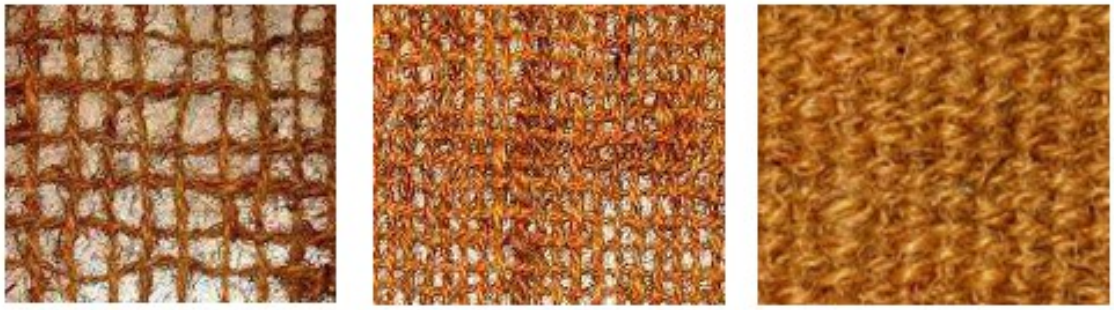

(a) (b) (c)

Figure 1. Coir geosynthetics types: (a) C1; (b) C2; (c) C3

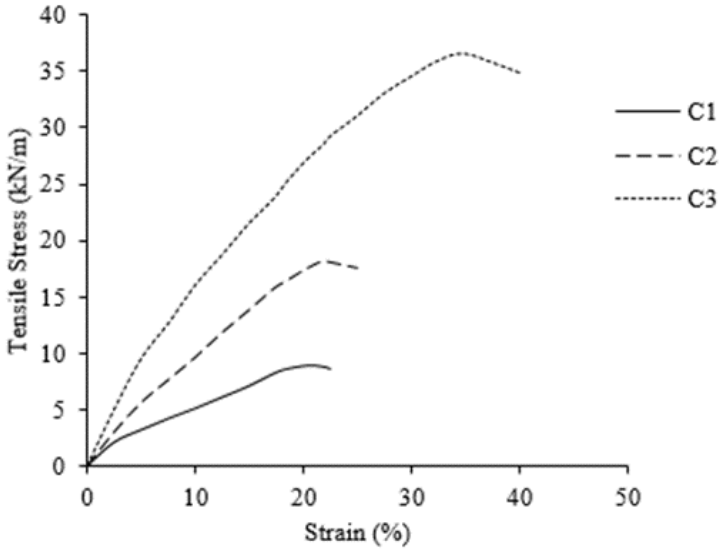

Figure 2. Tensile strength of coir geosynthetics

2.1.2 Pond ash

Pond ash was collected from the National Aluminium Company, Angul, Odisha (20.849°N, 85.154°E). Two types of pond ash, fine pond ash (FPA) and coarse pond ash (CPA), were selected for this study because of their distinct physical and mechanical properties, which can significantly influence the performance of pond ash reinforcement and other geotechnical

applications. By studying both types, a comprehensive understanding of how different particle sizes affect the soil stabilisation, load-bearing capacity, and settlement behaviour can be achieved. Figure 3 shows the particle size distribution of the pond ash. Some properties of pond ash are presented in Table 1, where NP denotes non-plastic.

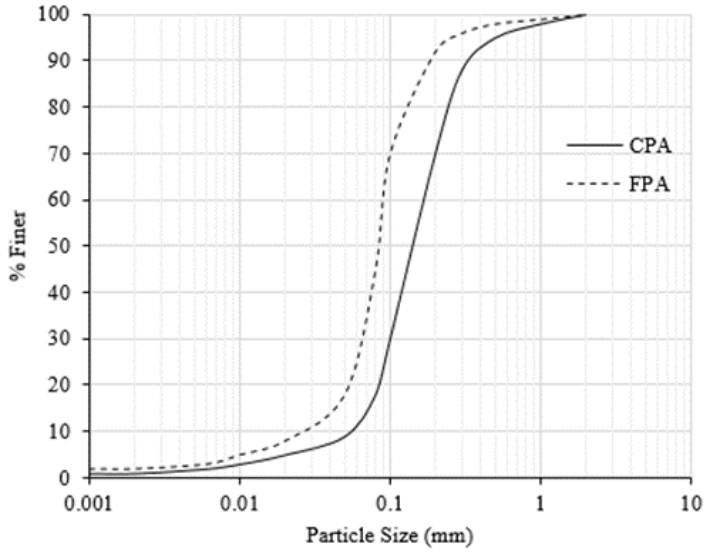

Figure 3. Particle size distribution of pond ash

Table 1. Physical characteristics, tensile strength, elongation at failure of woven coir geosynthetics and physical properties of pond ash

Parameter	Coir geosynthetics type			CPA	FPA	Standard
	C1	C2	C3			
Roll width (m)	1	1	1	--	--	[28]
Roll length (m)	50	50	24	--	--	[28]
Aperture size (mm × mm)	25 × 25	10,0 × 12,5	7,0 × 4,0	--	--	[28]
Thickness (mm)	6,5	7,8	9,2	--	--	[28]
Mass per unit area (g/m^2)	355	600	1325	--	--	[28]
Ultimate Tensile Strength (kN/m)	8,9	18,1	36,5	--	--	[29]
Elongation at Failure (%)	20,4	21,8	34,8	--	--	[29]
Specific Gravity	--	--	--	2,52	2,05	[30]
Liquid Limit (%)	--	--	--	35	43	[31]
Plastic limit (%)	--	--	--	NP	NP	[31]
MDD (kN/m^3)	--	--	--	13,47	9,89	[32]
Optimum moisture content (%)	--	--	--	24	33	[32]
Effective angle of internal friction (°) at MDD	--	--	--	34	32	[33]

Table 1 shows that CPA is denser and has larger and heavier particles than FPA, as indicated by its higher specific gravity. FPA has a higher liquid limit, meaning that it can absorb more moisture before becoming plastic, making it more susceptible to changes in consistency with the water content. Both types are non-plastic and behave like granular materials. CPA can be compacted to a higher density (greater MDD), making it more suitable for applications requiring high compaction. FPA, which has a larger surface area owing to its fine particles, requires

more moisture for compaction. The slightly higher angle of internal friction for CPA indicates better shear strength and stability when compacted compared with FPA.

2.2 Methods

2.2.1 Model tank

A model tank fitted with side plates was fabricated from 12 mm thick perspex, which was enclosed within a rigid mild steel frame. The internal dimensions of the tank were 750 x 750 x 400 mm (length x width x depth). The external dimensions of the tank were suitable for mounting on the Hounsfield Universal Testing equipment, which has a load capacity of 50 kN. An attached computer operated the machine and controlled the displacement and load on the crosshead. Having a maximum displacement of 1100 mm, the potential cross head rate ranged from 0,01-250,00 mm/min. Two tables were constructed using mild steel angles, one for loading and the other for compaction. After the compaction stage, the model tank was moved onto the machine and positioned on another table for loading.

2.2.2 Model studies on reinforced pond ash

Compact pond ash loaded with different geosynthetic materials was used for the model load tests. A strip footing with width B = 50 mm was mounted on the pond ash that had been compacted at the MDD with N geosynthetic layers. The uppermost geosynthetic layer was positioned at a depth of u from the base of the footing, with a separation of h between subsequent layers. Underneath the foundation, the width of the reinforced geosynthetic was b. The expression for the depth of reinforcement, d, underneath the footing is $d = u + (N - 1) \times h$.

The model experiments on reinforced CPA and FPA with geosynthetic types C1, C2, and C3 are shown in Figure 4. These studies included variables such as number of layers (N), layer depth from the base of the footing (u), and width of geosynthetic (b). Three different criteria were used for the model tests: (i) b/B = 5, N = 1 kept constant and u/B = 0,26; 0,40; 0,53; 0,66 as variables; (ii) u/B = 0,6; N =1 kept constant and b/B = 3; 5; 7; 9 as variables; and (iii) u/B = 0,4; b/B = 5; h/B = 0,33 kept constant and N = 1; 2; 3 as variables. The value of h = 16,5 cm for N = 2 and N = 3.

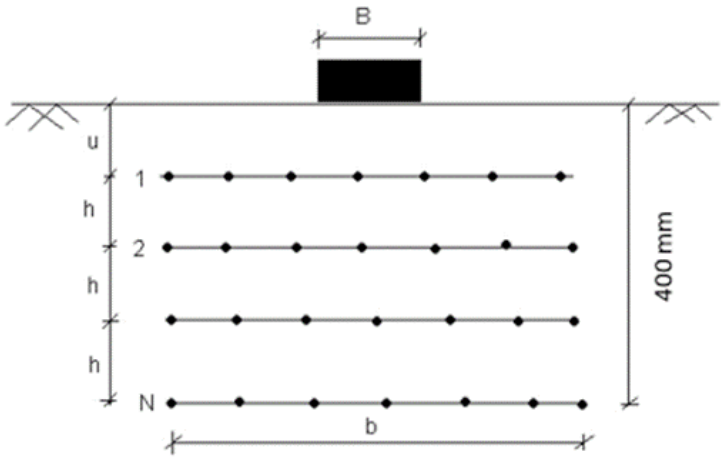

Figure 4. Model test footing

Figures 5 and 6 show the top view of the model tank at the end of loading, and the view of the coir geosynthetic reinforcement after the completion of loading.

Figure 5. Top view of model tank at the end of loading

Figure 6. Coir geosynthetics reinforcement after completion of loading

3 Results and discussions

3.1 Ultimate bearing capacity ratio

The unreinforced CPA had an ultimate bearing capacity (UBC) (q_u) of 265,4 kPa at a settlement (s_u) of 6,5 mm, whereas the unreinforced FPA had an UBC of 235.8 kPa at a settlement of 5,9 mm. Tables 2 and 3 list q_u and s_u for the two types of pond ash reinforced with various types of reinforcements. The ultimate bearing capacity ratio (BCR_u) was calculated to quantify the improvement in the load-bearing capacity owing to reinforcement. This is the ratio of the UBC of the reinforced pond ash to that of unreinforced pond ash. Tables 2 and 3 show that an increase in the number of reinforcements from one to three resulted in a considerable improvement in the BCR_u for both CPA and FPA.

The ratio b/B = 5 was selected based on the balance between ensuring adequate reinforcement within the effective load distribution zone and considering material cost-effectiveness. It was selected to simulate a scenario in which the reinforced zone covered a portion of the subgrade or embankment, ensuring sufficient load distribution without over-extending the geosynthetic material beyond its effective zone. When a wheel load was applied to the surface, it was distributed at an angle of 30° to the surface below. Installing geosynthetics

across the entire width of a road may not always be cost effective. By limiting the reinforcement to a ratio of *b/B* = 5, the design strikes a balance between reinforcement efficiency and material cost. This ensures that geosynthetics are applied where they are required without unnecessary overspreading.

Table 2. Variations in q_u and s_u for CPA

Factors			Criteria	q_u and s_u for CPA with N = 1, 2, 3					
				C1		C2		C3	
b/*B*	*u*/*B*	*N*		UBC q_u (kPa)	Settlement s_u (mm)	UBC q_u (kPa)	Settlement s_u (mm)	UBC q_u (kPa)	Settlement s_u (mm)
9	0,66	1	ii	384,2	8,3	424,2	10,1	390,5	10,7
7	0,66	1	ii	367,2	8,6	394,7	9,6	384,2	9,8
5	0,66	1	i, ii	349,1	8,3	374,9	9,2	357,9	10,3
3	0,66	1	ii	326,1	7,8	363,5	8,7	334,0	8,6
5	0,53	1	i	373,2	8,1	416,6	9,2	387,6	8,7
5	0,40	1	i	389,6	8,0	406,1	9,0	390,2	8,4
5	0,26	1	i, iii	382,0	7,8	384,8	8,7	378,6	8,1
5	0,40	2	iii	471,3	10,2	511,8	10,7	487,5	10,6
5	0,40	3	iii	602,6	12,6	746,6	13,3	672,9	12,9

Table 3. Variations in q_u and s_u for FPA

Factors			Criteria	q_u and s_u for FPA with N = 1, 2, 3					
				C1		C2		C3	
b/*B*	*u*/*B*	*N*		UBC q_u (kPa)	Settlement s_u (mm)	UBC q_u (kPa)	Settlement s_u (mm)	UBC q_u (kPa)	Settlement s_u (mm)
9	0,66	1	ii	359,5	9,2	393,1	9,8	377,8	10,2
7	0,66	1	ii	351,9	8,6	401,8	10,7	379,5	11,3
5	0,66	1	i, ii	351,6	8,2	382,0	9,6	361,8	11,2
3	0,66	1	ii	339,8	7,3	368,4	9,2	349,6	10,8
5	0,53	1	i	359,8	8,7	376,8	8,3	398,3	11,3
5	0,40	1	i	357,3	8,2	363,7	8,1	379,3	11,1
5	0,26	1	i, iii	334,1	7,5	339,3	7,8	351,6	10,6
5	0,40	2	iii	438,8	9,5	451,9	10,3	484,8	13,0
5	0,40	3	iii	517,7	11,0	598,5	12,4	643,9	15,2

The BCR_u values for the three types of reinforcements with CPA and FPA were computed and are listed in Tables 4 and 5 below. As shown in Figures 7a)-c) for CPA and Figures 8a)-c) for FPA, the values were reported in relation to the variable parameters *b/B*, *u/B*, and *N* to facilitate a clear comparison. The effects of the independent variables *b/B*, *u/B*, and *N* were investigated based on the BCR_u values. To simplify the comparison, the BCR_u values were plotted against b/B for both CPA and FPA with different types of reinforcements. The outcomes in Figures 7a) and 8a) reveal that for CPA with coir geosynthetics C1, C2, and C3, the BCR_u increases with b/B up to 9. In contrast, for FPA, the BCR_u values attained a maximum at a *b/B* value of 7 for coir geosynthetics types C2 and C3, after which there was a slight reduction in the value of BCR_u with a subsequent increase in the value of b/B.

Table 4. Variations in BCRu for CPA

Factors			BCR_u for CPA with N = 1, 2,3		
b*/*B	***u*/*B***	***N***	**C1**	**C2**	**C3**
9	0,66	1	1,45	1,60	1,47
7	0,66	1	1,38	1,49	1,45
5	0,66	1	1,32	1,41	1,35
3	0,66	1	1,23	1,37	1,26
5	0,53	1	1,41	1,57	1,46
5	0,40	1	1,47	1,53	1,47
5	0,26	1	1,44	1,45	1,43
5	0,40	2	1,78	1,93	1,84
5	0,40	3	2,27	2,81	2,54

Table 5. Variations in BCR_u for FPA

Factors			BCR_u for FPA with N = 1, 2, 3		
b*/*B	***u*/*B***	***N***	**C1**	**C2**	**C3**
9	0,66	1	1,52	1,67	1,60
7	0,66	1	1,49	1,70	1,61
5	0,66	1	1,49	1,62	1,53
3	0,66	1	1,44	1,56	1,48
5	0,53	1	1,53	1,60	1,69
5	0,40	1	1,52	1,54	1,61
5	0,26	1	1,42	1,44	1,49
5	0,40	2	1,86	1,92	2,06
5	0,40	3	2,20	2,54	2,73

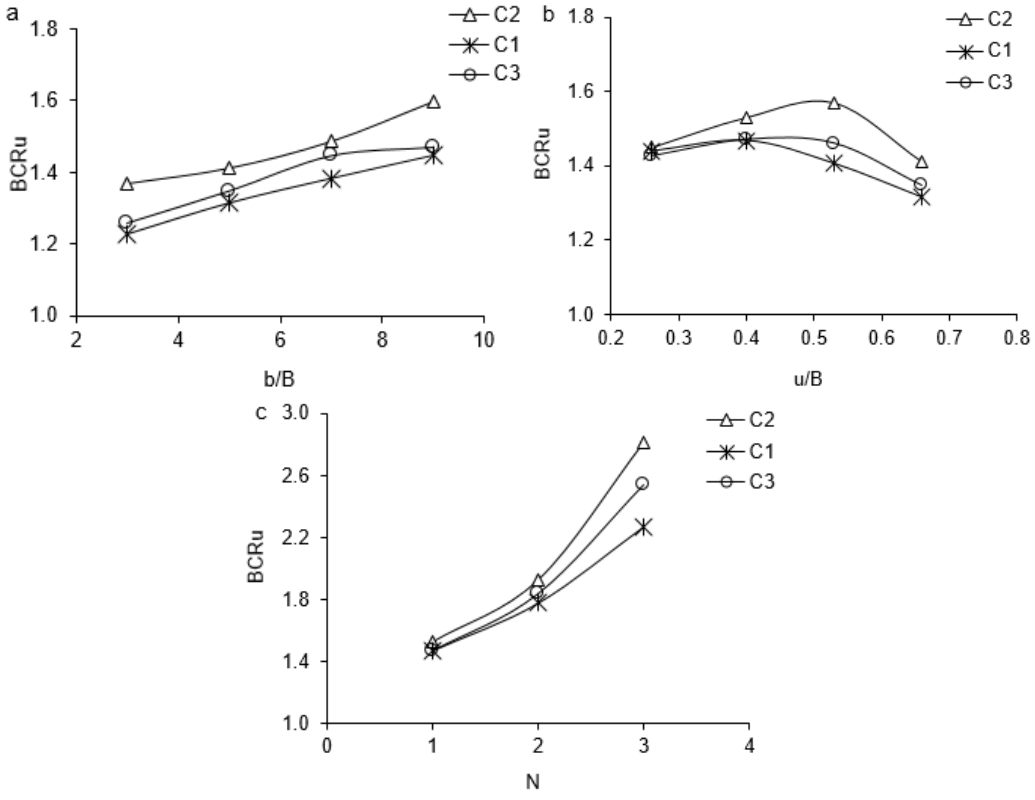

Figure 7. Variation of BCRu with different factors for CPA: a) *b/B*; b) *u/B*; c) *N*

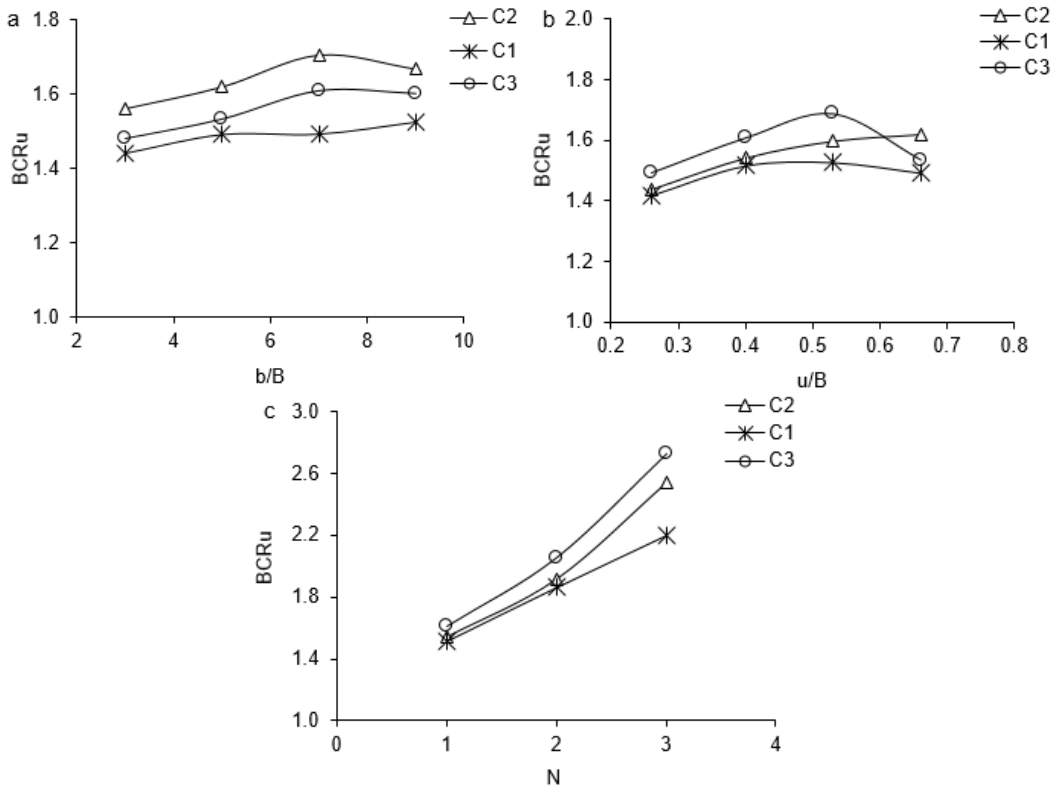

Figure 8. Variation of BCRu with different factors for FPA; a) *b/B*; b) *u/B*; c) *N*

When FPA and coir geosynthetic type C1 were used together, the value of BCR_u was consistent at 1,42 for *b/B* values of 5 and 7, and then increased slightly at a b/B value of 9. The BCR_u values first increased and then decreased with the addition of coir geosynthetics to both types of pond ash, as shown in Figures 7b) and 8b).

Figures 7c) and 8c) show the relationship between BCR_u and *N* for each scenario. For all types of pond ash and reinforcements, both figures indicate a significant enhancement in the BCR_u value with an increase in the number of reinforcement layers (*N*). All types of coir geosynthetics exhibited similar characteristics.

As Figures 7b) and 8b) show, the BCR_u values for CPA and FPA for different reinforcements often exhibit similar trends for the same values of *b/B* and *N*, as observed in a previous study [11].

3.1.1 Influence of u/B on BCR_u for CPA

Table 4 shows the changes to the BCR_u for CPA for constant b/B and *N* = 1 values: as *u/B* decreases from 0,66 to 0,26 for *b/B* = 5, the BCR values for C1, C2, and C3 show a relatively small variation, indicating a slight decrease or near-constant behaviour.

For lower values of *u/B*, the BCR_u cannot change significantly but tends to stabilise around constant values. There was a slight improvement in some cases such as at *u/B* = 0.53; however, overall, the influence was relatively small for the CPA when *N* = 1.

For *N* = 2 and 3, when *u/B* = 0,40 and *b/B* = 5, the BCR_u values for C1, C2, and C3 increase significantly as *N* increases. This shows that with more layers (increasing *N*), the BCR improved noticeably, which is consistent with the behaviour of more complex or multi-layered foundation conditions.

3.1.2 Influence of u/B on BCR_u for FPA

Table 5 shows the changes to the BCR_u for FPA for constant *b/B* and *N* = 1 values: as *u/B* decreases from 0,66 to 0,26 for *b/B* = 5, the BCR_u values for C1, C2, and C3 decrease. This

suggests that a decrease in *u/B* leads to a reduction in the BCR_u when *N* = 1, indicating that lower values of *u/B* correspond to weaker or less efficient foundation conditions.
The results for *N* = 2 and 3 suggest that under multiple layers, the bearing capacity improves with increasing *N*; however, the influence of u/B at these higher N values continues to play a significant role.
The tables and figures presented above demonstrate a substantial increase in the final bearing capacity of both types of pond ash after geosynthetics are used. The changing behaviour of BCR_u with respect to the values of *b/B* and *u/B* is significantly affected by the stiffness of the reinforcement type. Similarly, the weakest type of C1 coir geosynthetics demonstrated the least improvement across all combinations, as predicted. Surprisingly, when used as a single layer of reinforcement, coir geosynthetic type C2 outperformed type C3 with both types of pond ash. The tensile properties and aperture sizes of the two geosynthetics could have been partially responsible for this phenomenon. The coir geosynthetic type C2 had a larger aperture than type C3. As Figure 2 shows, for C1 geosynthetics, tensile stress increases gradually, reaching a peak of 8,9 kN/m at 20,4 % strain, followed by a slight reduction, indicating lower tensile strength and early strain-softening. C2 peaks at 18,1 kN/m at 21,8 % strain, showing higher tensile strength than C1 but also failing after a higher strain, with post-peak softening. C3 exhibits the highest tensile strength, peaking at 36,5 kN/m at 34,8 % strain. After reaching its maximum, C3 underwent strain softening but maintained a high stress over a wider strain range, exhibiting the most ductile behaviour and the ability to endure the largest strain before failure.

3.2 BCR at any settlement

Calculated at each settlement level, the BCRs were derived from the bearing capacity–settlement curves, which illustrated the correlation between the load-bearing capacity of the reinforced pond ash and the extent of settlement it experienced. Calculating the BCRs at different settlement levels provides a deeper understanding of how reinforcement enhances both the BCR_u and performance during intermediate loading stages, allowing for a comparison of different reinforcement configurations and their effectiveness in reducing settlement or increasing load-carrying capacity.
The results of this investigation are shown here as variations in the settlement ratio *s/B* (%), that is, the percentage representation of the ratio between the settlement and footing width. Figures 9a)-i) for the CPA with varying reinforcement and Figures 10a)-i) for the FPA show the variation in BCRs with *s/B*.
Generally, a high settlement is not feasible because the ultimate settlement occurs long before. As can be observed from Figures 10a)-i), the behaviours of the FPA and CPA are quite similar.

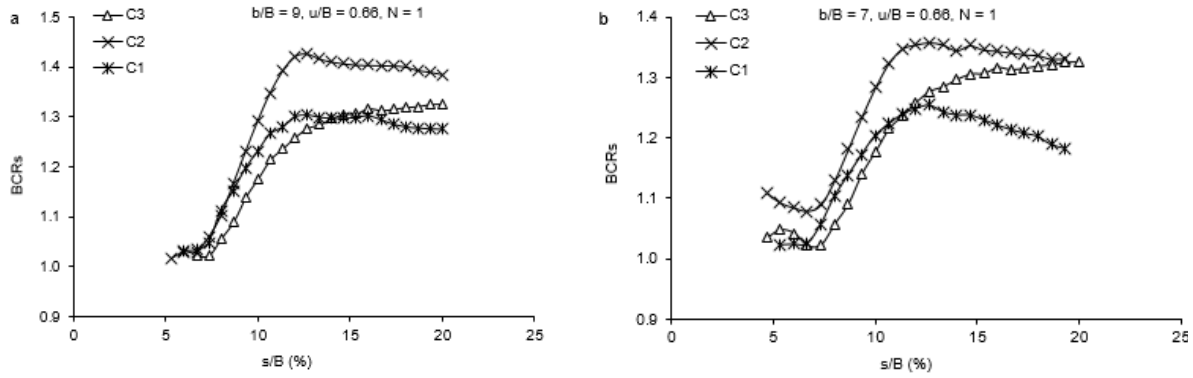

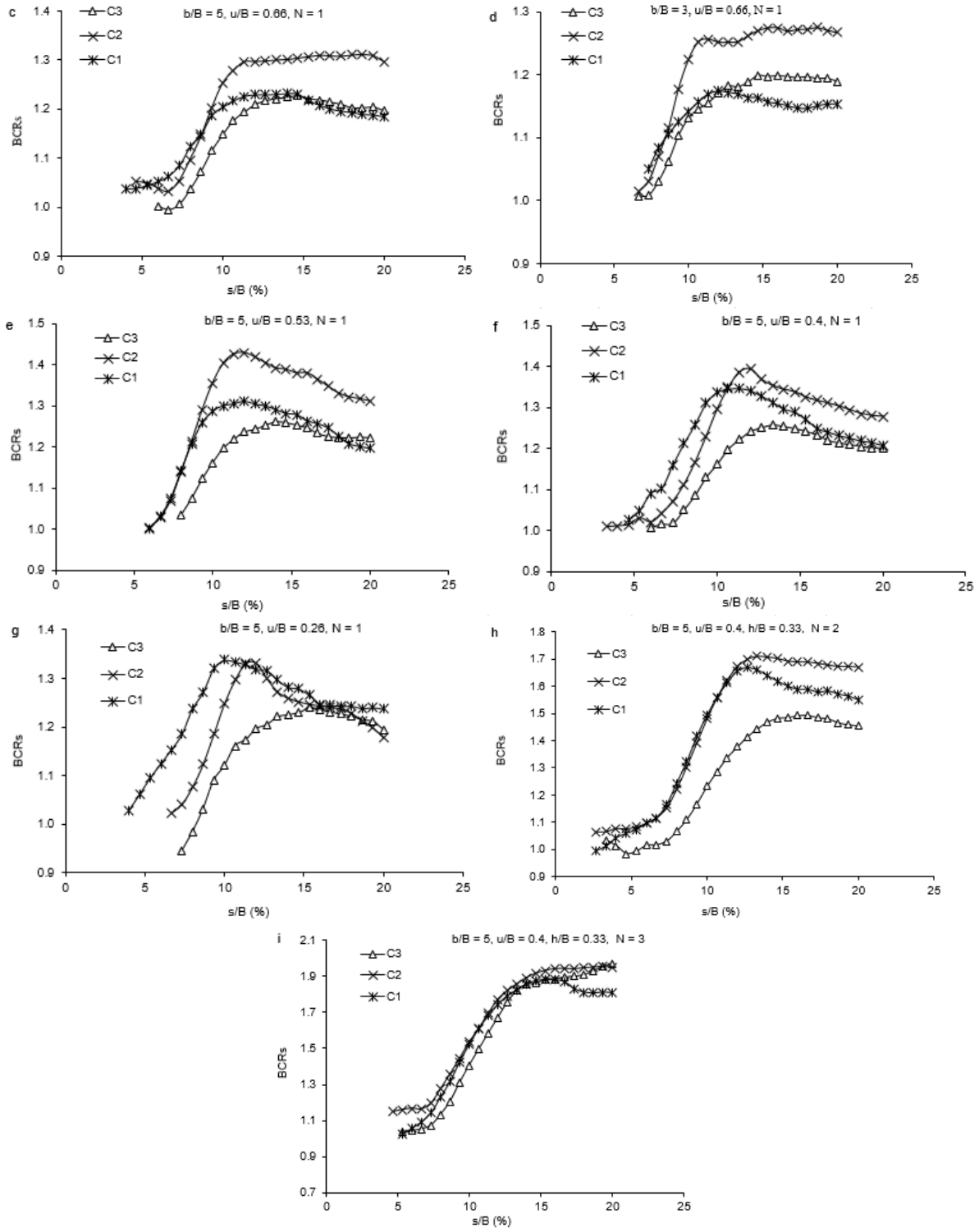

Figure 9. a)-i) Variations in BCR with s/B for CPA with varying reinforcement

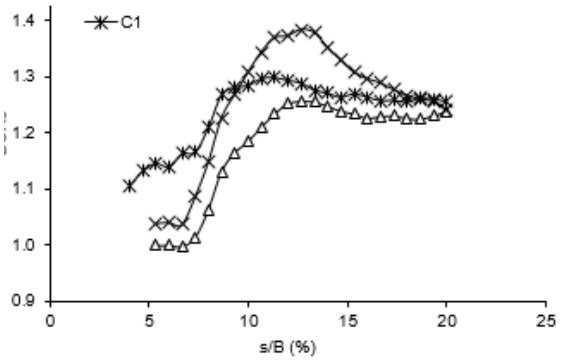
C1
s/B (%)

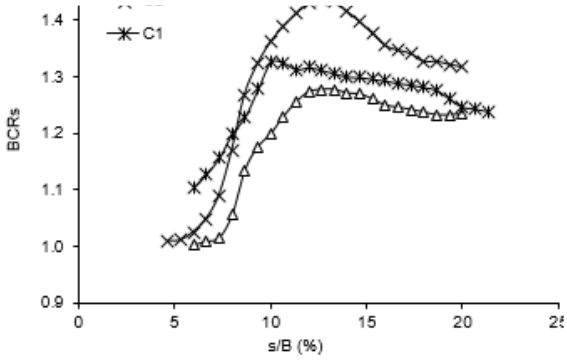
C1
BCRs
s/B (%)

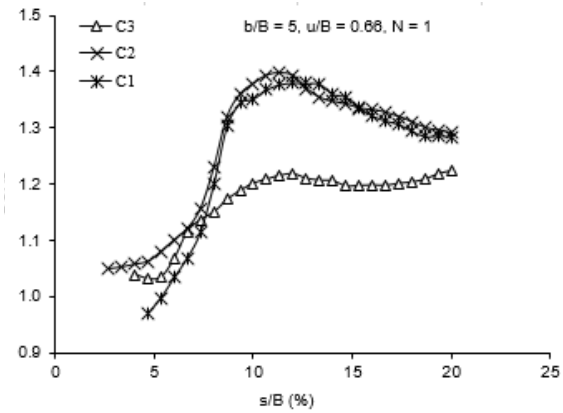
C3
C2
C1
b/B = 5, u/B = 0.66, N = 1
s/B (%)

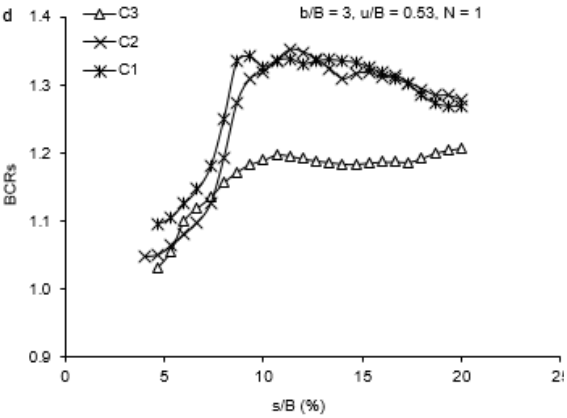
d
C3
C2
C1
b/B = 3, u/B = 0.53, N = 1
BCRs
s/B (%)

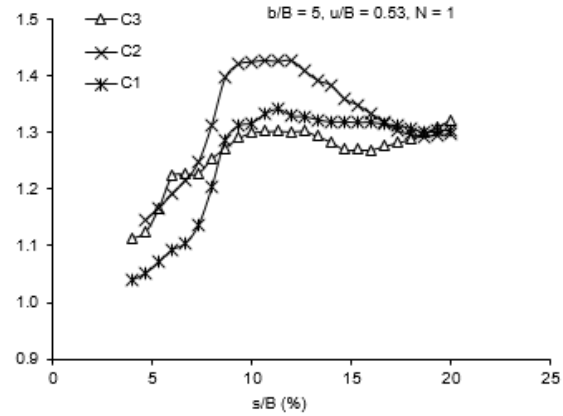
C3
C2
C1
b/B = 5, u/B = 0.53, N = 1
s/B (%)

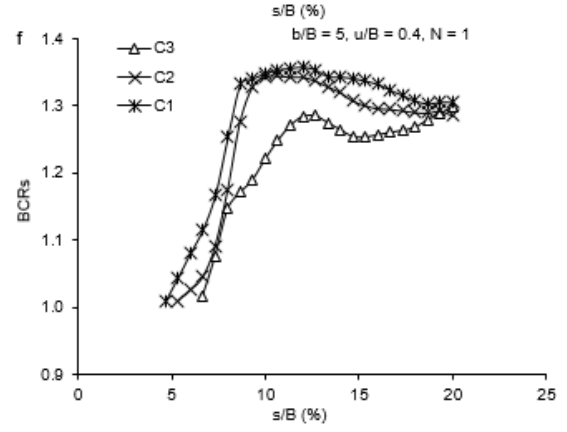
f
C3
C2
C1
b/B = 5, u/B = 0.4, N = 1
BCRs
s/B (%)

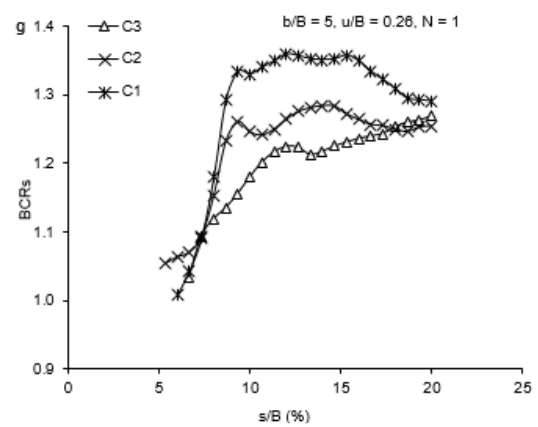
g
C3
C2
C1
b/B = 5, u/B = 0.26, N = 1
BCRs
s/B (%)

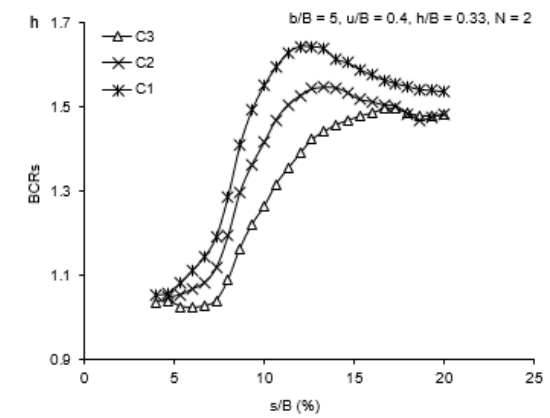
h
C3
C2
C1
b/B = 5, u/B = 0.4, h/B = 0.33, N = 2
BCRs
s/B (%)

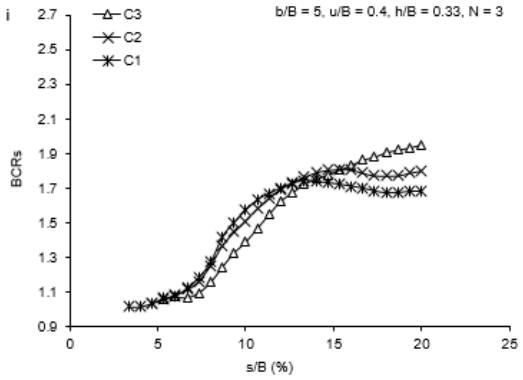

Figure 10. a)-i) Variations in BCR with s/B for FPA with varying reinforcement

Figures 9 and 10 show that for varying settling ratios, the BCR values for CPA vary according to a certain pattern with respect to *u/B*. For C3, the BCR_u values are < 1. This is because of the fibre waveform. Tension in the longitudinal direction perpendicular to the footing required time to develop when loaded. With the exception of C3, all of the reinforcements exhibited maximum BCR values at a settlement ratio of 12 %, with the highest found at a settlement ratio of 16 % for reinforcement type C3. The differences in the BCRs with *u/B* were significant for the FPA. After reaching its maximum value at *u/B* value of 0,53, the coir geosynthetic reinforcement (C1) exhibited a linear fluctuation for all settlement ratios. Subsequently, the values of the BCRs changed relatively little as s/B changed. At the *s/B* ratio of 12 %, the BCR values were almost identical to the BCR_u values across the board for *u/B* values. The u/B values of 0,53 for all s/B ratios were followed by a declining trend for the other coir geosynthetics, C2 and C3.

All the curves show that coir geosynthetic C3 acts differently from C1 and C2. The highest value of BCR_u was approximately 1,4; whereas the lowest value was approximately 1,25. A significant difference was observed between BCR_u and the BCRs of C3 and those of the other two coir geosynthetics, C1 and C2. This could be caused by the C3 type geosynthetics which have higher stress at higher elongation compared to the C1 and C2 geosynthetics.

Coir geosynthetics are not monolithic but are composed of individual fibres or strands woven together in a pattern. This woven structure allowed the fibres to pass over each other, creating a flexible material that stretched when subjected to tension. During this stretching the fibre within the weave reorients and adjusts, leading to higher elongation before the geosynthetic reaches its full tensile capacity. These characteristics render woven coir geosynthetics suitable for several different applications.

Each coir geosynthetic reinforcement, C1, C2, and C3, exhibits distinct patterns. For all settlement ratios, the BCR values exhibited an increasing pattern, which was closely correlated with an increase in *b/B*. Furthermore, the BCR values declined considerably when the settlement ratios were low for the coir geosynthetics.

The behaviour of FPA differed from that of CPA, as indicated by the BCR values. For both the CPA and FPA, the BCR curves were almost always steep for all settlements. However, at higher *s/B* ratios, there was no change. However, it is not immediately apparent why this discrepancy occurred.

Compared with C1 and C2, a significant difference was observed in the top two BCR and BCR_u curves. In the stress–strain relationship, the C3 type geosynthetics have a higher stress at higher elongation than the C1 and C2 geosynthetics.

Furthermore, for all settlement ratios, the BCR values were constant after *b/B* = 5. However, a peak value of the BCR exists at *b/B* = 7 for all settlement ratios. A clear and identifiable pattern was observed for coir geosynthetic reinforcements C1, C2, and C3. At all settlement ratios, the BCR values consistently exhibited an upward trend in conjunction with an increase in b/B.

In addition, the coir geosynthetics' BCR_u curves are higher than the BCR curves. In the reinforced case, the vertical settlement was lower than that in the unreinforced case. This is

because reinforcement materials (e.g., geosynthetics or coir geosynthetics) improve the load distribution and enhance the ability of the soil to resist deformation under applied loads. Reinforcement reduces the compressibility of the soil, limits the vertical settlement, and increases the overall stability of the structure.
Increasing the number of reinforcing layers significantly increased the BCR values for all settlement ratios. With increasing s/B ratios, the BCR curves for coir geosynthetic types C1 and C2 were comparable to one another. However, for coir geosynthetic type C3, the BCR values increased as the *s/B* and *N* values increased. Comparable BCR fluctuations with N were observed for all the types of reinforcements in FPA.
A comparison of the bearing capacity ratios at any settlement (BCRs) was performed with the findings published in a previous study [11] on pond ash reinforced with jute geosynthetics, just as in the case of the BCR_u of reinforced pond ash with either polymeric geosynthetics or coir geosynthetics and found to be similar to the present study.

4 Mathematical models

A multiple regression analysis was performed for the CPA and FPA, to develop a mathematical model. To create a model for any type of pond ash, the tangent of the angle of internal friction (Φ) has been considered. Of the 54 sets of data, 48 were used to develop the models (Equations (1) and (2)), and the remaining six sets of randomly chosen data were used to validate the proposed mathematical model (Equation (3)).
For each test result of the investigation of reinforced pond ash, data regression analysis was performed. By applying a multiple regression analysis, two different models were developed for each type of pond ash. The model for CPA is:

$$\mathrm{BCR_u} = 1{,}4036 + 0{,}0344(b/B) - 1{,}8137(u/B) + 1{,}5926(d/B) - 0{,}0933(t) \quad (1)$$

Where *t* denotes strength ratio between 2-5 % strain obtained from the tensile stress–strain curve of the reinforcements (2 and 5% strain levels are often chosen because they help illustrate the performance of the material at both early deformation stages (2%) and moderate deformation stages (5%)). This is valuable for understanding the mechanical behaviour of the material, especially for reinforced materials such as pond ash, where reinforcement may alter the response to stress at different strain levels.
The coefficient of determination (R^2) of the model was 0,9248. Similarly, the model developed for FPA with R^2 = 0,9208:

$$\mathrm{BCR_u} = 0{,}9439 + 0{,}0153(b/B) - 1{,}2732(u/B) + 1{,}4482(d/B) + 0{,}7362(t) \quad (2)$$

For general pond ash, the following mathematical model is suggested with R^2 = 0,91:

$$\mathrm{BCR_u} = 2{,}4839 + 0{,}0249(b/B) - 1{,}5434(u/B) + 1{,}5204(d/B) + 0{,}3214(t) - 2{,}0174(tan\phi) \quad (3)$$

Figures 11 and 12 show the variation between the test results and outcomes predicted based on Equations (1) and (2). Figures 13 and 14 compare the experimental (observed) and projected levels of BCR_u for CPA and FPA, respectively.

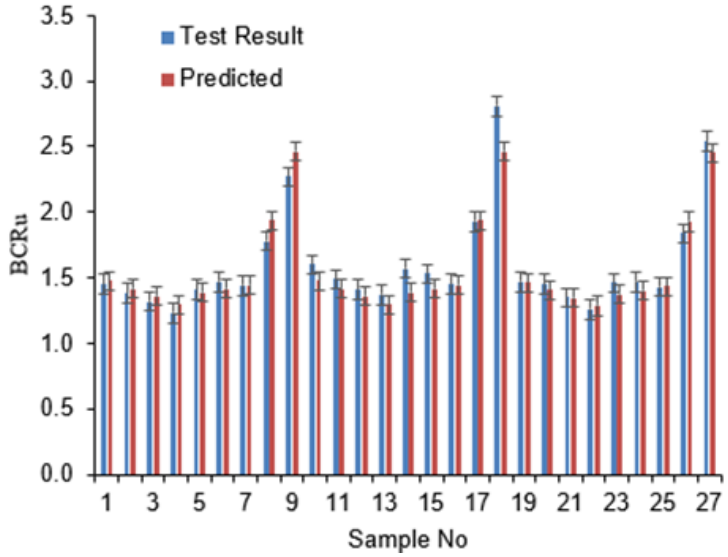

Figure 11. Test and predicted values of BCR_u for CPA using Equation (1)

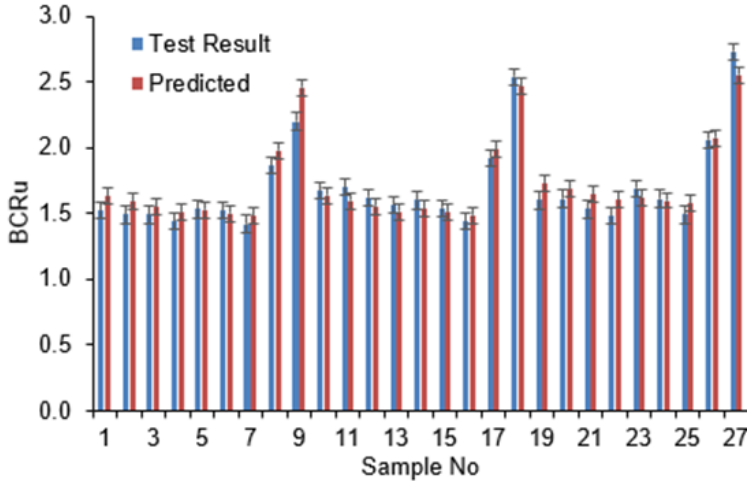

Figure 12. Test and predicted values of BCR_u for FPA using Equation (2)

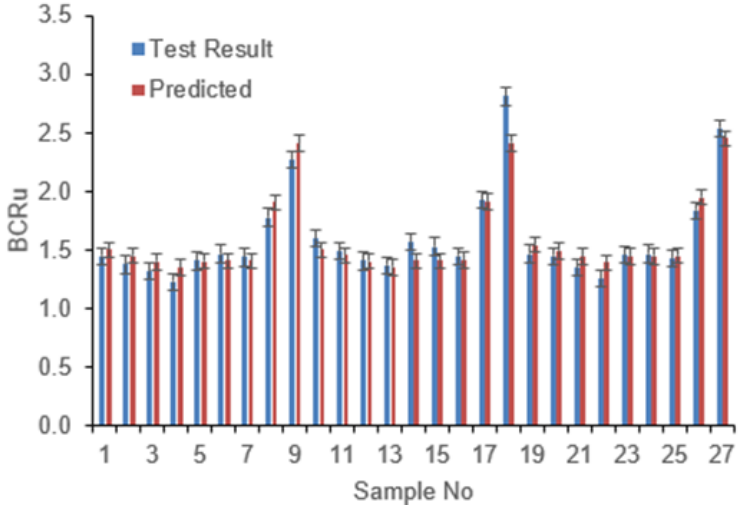

Figure 13. Test and predicted values of BCR_u for CPA using Equation (3)

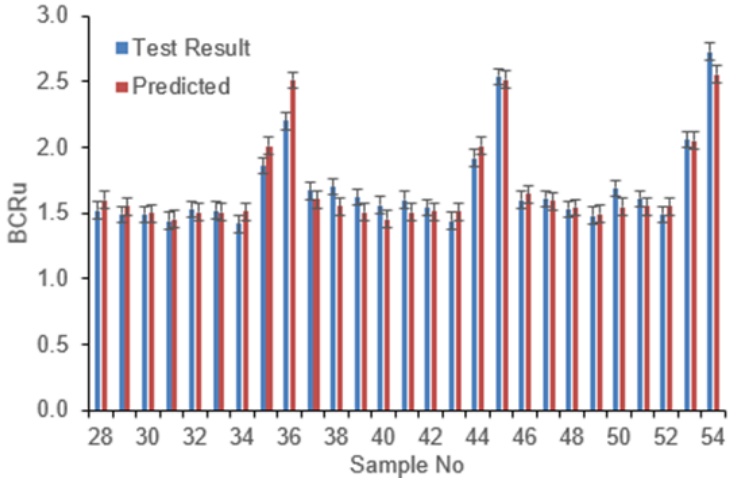

Figure 14. Test and predicted values of BCR_u for FPA using Equation (3)

An analysis of the expected and observed BCR_u values is presented in Figure 15. The analysis revealed a significant relationship between the measured and predicted levels of BCR_u.

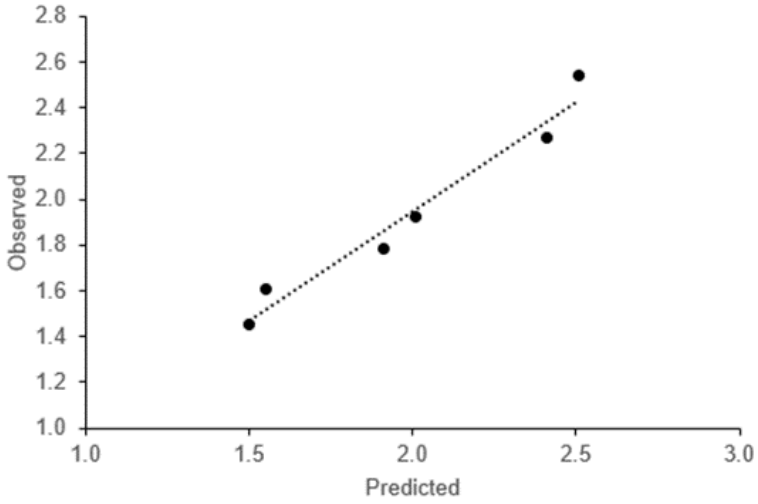

Figure 15. Test and predicted values of BCR_u for CPA and FPA using Equation (3)

5 Conclusions

Based on the test results, the following conclusions were drawn:

- By incorporating coir-woven geosynthetics, the ultimate bearing capacity significantly improved.
- For lower values of *u/B*, the BCR does not change dramatically but tends to stabilise around constant values. A decrease in *u/B* decreased the BCR for FPA. With multiple layers, the bearing capacity improved with increasing *N* for both CPA and FPA.
- The *b/B* ratio is inversely proportional to the BCR. As *b/B* increases (i.e., the footing becomes wider in proportion to B), the BCR tends to increase, leading to higher C1, C2, and C3 values for the CPA. As b/B decreased (for example, from 9 to 3), the values of the bearing capacity factors C1, C2, and C3 tended to decrease slightly for the FPA.
- Increasing N significantly improved the BCR, particularly for intermediate *b/B* values such as 5.

- The BCR at any settlement for the two types of pond ash combined with the geosynthetic woven from coir demonstrated an improved performance at higher settlements.
- Owing to its poor mechanical and physical qualities, coir geosynthetic type C1 showed the least improvement.
- In every test combination, coir geosynthetic type C2 performed better for CPA, which was coarser.
- When using a single layer of reinforcement with FPA, the C2 and C3 types of coir geosynthetics exhibited mixed results; however, when using multiple layers of reinforcement, C3 performed better.
- Some Coir geosynthetics exhibited high BCRs at higher settlements due to their weaving pattern.
- The regression analysis model derived from the model test results can be used to predict the BCR_u.

References

[1] Government of India – Ministry of Road Transport and Highways Transport Research Wing New Delhi. Basic road statistics 2018-19. Accessed: March 30, 2025. Available at: https://morth.nic.in/sites/default/files/Basic%20Road%20Statistics%20in%20India-2018-19.pdf

[2] Central Electricity Authority (CEA). Annual Report on Fly Ash Generation at Coal/Lignite Based Thermal Power Stations. Accessed: March 30, 2025. Available at: https://cea.nic.in/wp-content/uploads/tcd/2023/05/Half_Yearly_Ash_Report_2022_23.pdf

[3] Pradhip, V. P.; Balu, S.; Subramanian, B.; Subramanian, B. Pond ash as a potential material for sustainable geotechnical applications – a review. *Environmental Science and Pollution Research*, 2023, 30, pp. 102083-102103. https://doi.org/10.1007/s11356-023-29671-7

[4] Koerner, R. M.; Hwu, B.-L.; Wayne, M. H. Soft soil stabilization designs using geosynthetics. *Geotextiles and Geomembranes*, 1987, 6 (1-3), pp. 33-51. https://doi.org/10.1016/0266-1144(87)90056-2

[5] Lackner, C.; Bergado, D. T.; Semprich, S. Prestressed reinforced soil by geosynthetics—Concept and experimental investigations. *Geotextiles and Geomembranes*, 2013, 37, pp. 109-123. https://doi.org/10.1016/j.geotexmem.2013.02.002

[6] Chaiyaput, S.; Bergado, D. T.; Artidteang, S. Measured and simulated results of a Kenaf Limited Life Geosynthetics (LLGs) reinforced test embankment on soft clay. *Geotextiles and Geomembranes*, 2014, 42 (1), pp. 39-47. https://doi.org/10.1016/j.geotexmem.2013.12.006

[7] Boushehrian, A. H.; Hataf, N.; Ghahramani, A. Modeling of the cyclic behavior of shallow foundations resting on geomesh and grid anchor reinforced sand. *Geotextiles and Geomembranes*, 2011, 29 (3), pp.242-248. https://doi.org/10.1016/j.geotexmem.2010.11.008

[8] Bai, X.-H.; Huang, X.-Z.; Zhang, W. Bearing capacity of square footing supported by a geobelt-reinforced crushed stone cushion on soft soil. *Geotextiles and Geomembranes*, 2013, 38, pp. 37-42. https://doi.org/10.1016/j.geotexmem.2013.04.004

[9] Plé, O.; Lê, T. N. H. Effect of polypropylene fiber-reinforcement on the mechanical behavior of silty clay. *Geotextiles and Geomembranes*, 2012, 32, pp. 111-116. https://doi.org/10.1016/j.geotexmem.2011.11.004

[10] Lal, D.; Sankar, N.; Chandrakaran, S. Effect of reinforcement form on the behaviour of coir geotextile reinforced sand beds. *Soils and Foundations*, 2017, 57 (2), pp. 227-236. https://doi.org/10.1016/j.sandf.2016.12.001

[11] Ghosh, A.; Ghosh, A.; Bera, A. K. Bearing capacity of square footing on pond ash reinforced with jute-geotextile. *Geotextiles and Geomembranes*, 2005, 23 (2), pp.144-173. https://doi.org/10.1016/j.geotexmem.2004.07.002
[12] Madhavi Latha, G.; Murthy, V. S. Effects of reinforcement form on the behavior of geosynthetics reinforced sand. *Geotextiles and Geomembranes*, 2007, 25 (1), pp. 23-32. https://doi.org/10.1016/j.geotexmem.2006.09.002
[13] Moghaddas Tafreshi, S. N.; Dawson, A. R. Comparison of bearing capacity of a strip footing on sand with geocell and with planar forms of geotextile reinforcement. *Geotextiles and Geomembranes*, 2010, 28 (1), pp. 72-84. https://doi.org/10.1016/j.geotexmem.2009.09.003
[14] Sivakumar Babu, G. L.; Vasudevan, A. K.; Sayida, M. K. Use of coir fibers for improving the engineering properties of expansive soils. *Journal of Natural Fibers*, 2008, 5 (1), pp. 61-75. https://doi.org/10.1080/15440470801901522
[15] Widianti, A.; Diana, W.; Alghifari, M. R. Shear strength and elastic modulus behavior of coconut fiber-reinforced expansive soil. *IOP Conference Series: Materials Science and Engineering*, 2021, 1144, 012043. https://doi.org/10.1088/1757-899x/1144/1/012043
[16] Yang, H. et al. The strength law of coir fiber-reinforced soil based on modified Duncan-Chang model. *Frontier in Earth Science*, 2022, 10, 1078624. https://doi.org/10.3389/feart.2022.1078624
[17] Fang, K. et al. Centrifuge modelling of landslides and landslide hazard mitigation: A review. *Geoscience Frontiers*, 2023, 14 (1), 101493. https://doi.org/10.1016/j.gsf.2022.101493
[18] Lekha, K. R.; Kavitha, V. Coir geotextile reinforced clay dykes for drainage of low-lying areas. *Geotextiles and Geomembranes*, 2006, 24 (1), pp. 38-51. https://doi.org/10.1016/j.geotexmem.2005.05.001
[19] Vinod, P.; Minu, M. Use of coir geotextiles in unpaved road construction. *Geosynthetics International*, 2010, 17 (4), pp. 220-227. https://doi.org/10.1680/gein.2010.17.4.220
[20] Vinod, P.; Bhaskar, A. B.; Sreehari, S. Behaviour of a square model footing on loose sand reinforced with braided coir rope. *Geotextiles and Geomembranes*, 2009, 27 (6), pp. 464-474. https://doi.org/10.1016/j.geotexmem.2009.08.001
[21] Vinod, P.; Bhaskar, A.; Lekshmi, C. S. Triaxial compression of clay reinforced with sand-coir fiber core. *Geotechnical Testing Journal*, 2007, 30 (4), pp. 333-336. https://doi.org/10.1520/GTJ12639
[22] Noorzad, R.; Mirmoradi, S. H. Laboratory evaluation of the behavior of a geotextile reinforced clay. *Geotextiles and Geomembranes*, 2010, 28 (4), pp. 386-392. https://doi.org/10.1016/j.geotexmem.2009.12.002
[23] Dash, S. K.; Krishnaswamy, N. R.; Rajagopal, K. Bearing capacity of strip footing supported on geocell reinforced sand. *Geotextiles and Geomembranes*, 2001, 19 (4), pp. 235-256. https://doi.org/10.1016/S0266-1144(01)00006-1
[24] Sharma, A.; Nallasivam, K. Comparison of Bearing Capacity Behavior of Strip Footing Resting on Sand-Admixed Pond Ash Reinforced with Natural Fiber and Geogrid. *Indian Geotechnical Journal*, 2003, 53, pp. 1262-1279. https://doi.org/10.1007/s40098-023-00745-0
[25] Guo, X.; Zhang, H.; Liu, L. Planar geosynthetic-reinforced soil foundations: a review. *SN Applied Sciences*, 2020, 2, 2074. https://doi.org/10.1007/s42452-020-03930-5
[26] Pradhan, S. K.; Pothal, G. K. Experimental and cost evaluation of pond ash reinforced with polymeric geogrid. *Multiscale and Multidisciplinary. Modelling Experiments and Design*, 2023, 7, pp. 349-363. https://doi.org/10.1007/s41939-023-00214-4
[27] Pradhan, S. K.; Pothal, G. K. Shear Strength Characteristics of Pond Ash Reinforced with Polymeric and Natural Fiber Geosynthetic. *Geotechnical and Geological Engineering*, 2024, 42, pp. 3897-3918. https://doi.org/10.1007/s10706-024-02765-w
[28] Bureau of Indian Standards. IS 15868-1 to 6. *Natural fibre geosynthetics (jute geosynthetics and coir bhoovastra) - Methods of test*. New Delhi: IS; 2008.

[29] Bureau of Indian Standards. IS 1969-1. *Textiles - Tensile Properties of Fabrics - Determination of Maximum Force and Elongation at Maximum Force, Part 1: Strip Method*. New Delhi: IS; 2009.
[30] Bureau of Indian Standards. IS 2720-3-1. *Methods of test for soils, Part 3: Determination of specific gravity, Section 1: Fine grained soils*. New Delhi: IS; 1980.
[31] Bureau of Indian Standards.IS 2720-5. *Methods of test for soils, Part 5: Determination of liquid and plastic limit*. New Delhi: IS; 1985.
[32] Bureau of Indian Standards. IS 2720-7. *Methods of test for soils, Part 7: Determination of water content-dry density relation using light compaction*. New Delhi: IS; 1980.
[33] Bureau of Indian Standards. IS 2720-13. *Methods of test for soils, Part 13: Direct shear test*. New Delhi: IS; 1986.